Accepted Manuscript

Novel triphenylamine-based fluorescent probe for specific detection and bioimaging of OCl^-

Yuliang Jiang, Sheng Zhang, Bingxiang Wang, Tao Qian, Can Jin, Shishan Wu, Jian Shen

PII: S0040-4020(18)30961-X

DOI: 10.1016/j.tet.2018.08.010

Reference: TET 29730

To appear in: *Tetrahedron*

Received Date: 7 June 2018

Revised Date: 18 July 2018

Accepted Date: 10 August 2018

Please cite this article as: Jiang Y, Zhang S, Wang B, Qian T, Jin C, Wu S, Shen J, Novel triphenylamine-based fluorescent probe for specific detection and bioimaging of OCl^-, *Tetrahedron* (2018), doi: 10.1016/j.tet.2018.08.010.

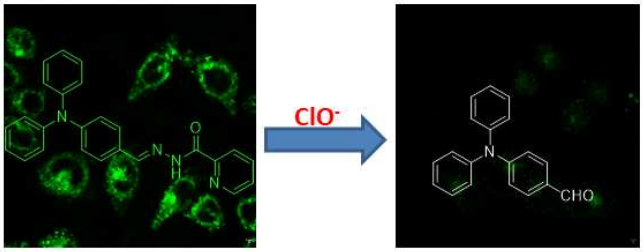

Novel triphenylamine-based fluorescent probe for specific detection and bioimaging of OCl^-

Yuliang Jiang[a], Sheng Zhang[a], Bingxiang Wang[a], Tao Qian[d], Can Jin[b]*, Shishan Wu[c]*, Jian Shen[a,c]*

a. Jiangsu Collaborative Innovation Center of Biomedical Functional Materials, Nanjing Normal University, Nanjing 210023, China

b. Institute of Chemical Industry of Forest Products, Chinese Academy of Forestry, Key Laboratory of Biomass Energy and Material of Jiangsu Province, Nanjing 210042, China

c. School of Chemistry and Chemical Engineering, Nanjing University, Nanjing 210093, China

d. Soochow Institute for Energy and Materials Innovations, College of Physics, Optoelectronics and Energy & Collaborative Innovation Center of Suzhou Nano Science and Technology, Soochow University, Suzhou 215006, China

Corresponding Authors

Email: envis@163.com (C. Jin), shishanwu@nju.edu.cn (S. Wu), jshen@njnu.edu.cn (J. Shen)

Abstract:

Hypochlorite (OCl^-) plays important roles both in physiological and pathological processes, the detection of which is of great significance. Herein, a novel fluorescent probe based on the triphenylamine-type schiff base derivative (TPAD) was developed to detect OCl^-. Probe TPAD exhibited specific fluorescence response toward ClO^- with the fluorescence quenching rate up to 80%, and the detection limit was estimated to be 0.8 μM. The sensing mechanism study demonstrated that TPAD reacted with ClO^- *via* an oxidation process, which was evidenced by MS and NMR characterization. Moreover, owing to the excellent sensing properties and negligible cytotoxicity, TPAD was successfully applied in the bioimaging of OCl^- in living A549 cells.

Keywords: Hypochlorite; Detection limit; Triphenylamine; Fluorescence probe; Cell imaging

Introduction

Reactive oxygen species (ROS) play crucial roles in many physiological and pathological processes.[1-3] As one of the most important ROS in living body, hypochlorite (OCl^-) is generally produced in organisms from the myeloperoxidase

(MPO) mediated peroxidation of chloride ions and hydrogen peroxide, which plays an important role in immune system against inflammation and microorganisms.[4] Owing to its high reactivity and nonspecificity in physiological conditions, excessive or misplaced production of OCl^- level could cause harmful chain effects to human beings, including neuron degeneration,[5] cardiovascular disease,[6] lung injury,[7] atherosclerosis,[8] and cancers.[9-11] Therefore, highly sensitive and selective detection of short-lived OCl^- in living systems is meaningful and has attracted increasing attention.[12, 13]

Fluorescent sensing strategy has been demonstrated as an ideal tool for OCl^- detection in both chemical sensing and biological imaging thanks to its high sensitivity, low cost and technical simplicity.[14-18] Recently, a large number of fluorescent probes have been exploited by utilizing specific recognition units to distinguish $HOCl/OCl^-$ from other ROS species, including p-methoxyphenol,[19] oxime,[20] selenide,[21] thiol[22, 23] and other functional groups (e.g. nanomaterial).[24-26] Nevertheless, many of these probes might encounter some issues, such as delayed response,low sensitivity and requiring multi-step synthetic operation. Meanwhile, due to the typical characteristics of OCl^- is highly reactive, short-lived under physiological conditions, rapid response and high sensitivity is mostly desirable for real-time monitoring of OCl^- fluctuation. Thus, it is eagerly desirable but still highly challenging to design and develop advanced probes with high sensitivity, high selectivity and rapid-response properties for real-time detection of low-concentration endogenous OCl^- in living biological systems through simple synthesis.

Triphenylamine as an ideal molecule matrix has been widely used in the construction of opto- and electro-active materials owing to its molecular non-coplanarity, vibronic coupling and high stability.[27-29] However, the use of triphenylamine for fluorescent probes has not received a lot of attention. In order to explore the application of this matrix in fluorescent probes field, herein, we have designed and synthesized a novel triphenylamine-type schiff base derivative (TPAD) for the spectic detection of OCl^- by one-step synthetic process from picolinohydrazide

and 4-(diphenylamino)benzaldehyde (Scheme 1). The probe TPAD exhibited selective, sensitive and rapid response to OCl^-, which was determined by fluoresence spectroscopy. Furthermore, the bioimaging application of probe TPAD for OCl^- detection in living cells was also investigated.

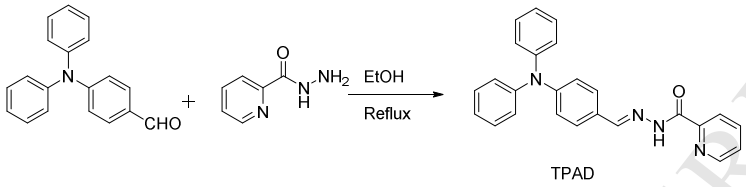

Scheme 1. Synthesis route of TPAD probe

2. Experimental

2.1. Chemicals and apparatus

Triphenylamine, picolinohydrazide, hydrogen peroxide, sodium hypochlorite, and 3-(4,5-dimethylthiazol-2-yl)-2,5-diphenyltetrazoliumbromide (MTT) were purchased from Aladdin Chemistry Co. Ltd (Shanghai, China) and used without further purification. Ethanol and DMSO were analytical pure and distilled before used. Various testing species including CO_3^{2-}, $H_2PO_4^-$, Cl^-, H_2O_2, OCl^-, $TBuO^-$, HO^-, $^1O_2$, NO, $ONOO^-$ and NO_2^- were prepared in solutions according to the following methods, respectively: T-BuO^- from Aladdin Co. Ltd was diluted to the required concentration; HO^- was generated from Fenton reaction between Ferrous solution; $^1O_2$ was produced via the reaction of H_2O_2 with NaOCl; NO is emitted from 3-(Aminopropyl)-1-hydroxy-3-isopropyl-2-oxo-1-triazene (NOC-5); $ONOO^-$ source was replaced by the 3-morpholinosydnonimine hydrochloride (SIN-1, 50.0 μM); The source of NO_2^- was obtained from $NaNO_2$. All other ion salts were purchased from Nanjing Chemical Reagent Co., Ltd. (Nanjing, China). Double-distilled water was used throughout all the experimental solutions. All samples were prepared at room temperature and were shaken for 1 min before each experiment.

^1H NMR and ^{13}C NMR spectra of samples were recorded on an AVANCE III HD AN-400 MHz spectrometer (Bruker, Germany) with TMS as an internal standard. Ultraviolet-Visible (UV-vis) absorption spectra were measured on a Varian Cary 50

spectrophotometer (Agilent, USA) at 1 cm of the light path length. Fluorescence spectra were recorded on a Varian cary eclipse fluorescence spectrophotometer (Agilent, USA) with an excitation wavelength of 375 nm. Mass spectroscopy data of the samples were collected on a LCMS-2020 spectrometer (Shimadzu, Japan). Element analysis of samples was operated on a PE 2400 elemental analyzer (PerkinElmer, USA). All fluorescence imaging experiments were conducted using a A1 confocal laser scanning microscope (Nikon, Japan).

2.2. Synthesis of TPAD

4-(diphenylamino)benzaldehyde was prepared according to the reported literature.[30] TPAD was conveniently synthesized following the synthetic route (Scheme 1). 0.273 g 4-(diphenylamino)benzaldehyde (1.0 mmol) was dissolved in 20 mL ethanol solution, then 0.137 g picolinohydrazide (1.0 mmol) was added into the solution and the mixture was heated at reflux and stirred for 12 h. After the reaction system was cooled to room temperature, a yellow precipitate was obtained and collected by filtration, washed with cold ethanol and dried in vacuum to afford probe TPAD as a yellow powder (87% yield, 0.196 g). ^{1}H NMR (400 MHz, DMSO-d_6), δ (ppm): 12.06 (s, 1H), 8.80-8.64 (m, 1H), 8.57 (s, 1H), 8.16-7.97 (m, 2H), 7.72-7.52 (m, 3H), 7.36 (t, J = 7.8 Hz, 4H), 7.12 (dd, J_1 = 17.7, J_2 = 7.5 Hz, 6H), 6.98 (d, J = 8.6 Hz, 2H). ^{13}C NMR (100 MHz, DMSO-d_6), δ (ppm): 159.78 , 150.08, 149.30, 148.74, 147.98, 147.01, 137.71, 129.49, 128.94, 126.66, 125.35, 123.92, 122.92, 121.70. MS (ESI) calculated for $[M+1]^+$ 393.06, found 393.09. Elemental analysis (%) calculated for $C_{25}H_{20}N_4O$: C, 76.51; H, 5.14; N, 14.28; found: C, 76.48; H, 5.12; N, 14.30. (^{1}H NMR, ^{13}C NMR and ESI spectra of TPAD could be found in Fig. S1−S3).

2.3. UV–vis and fluorescence analysis

Double-distilled water and analytical purity DMSO were used to prepared solvent for the absorption spectra studies. Compound TPAD was dissolved in DMSO/PBS buffer solution (1:4, V/V, 10 mM PBS buffer, pH 7.4) to afford a stock solution in 10 mM concentration. Solutions of various testing species were prepared by dilution of the stock solution with PBS buffer solution. The resulting solutions

were well shaken and incubated for 1 h at room temperature before spectra data recording.

2.4. Cytotoxicity studies

The methyl thiazolyl tetrazolium (MTT) assay was used to measure the cytotoxicity of TPAD in A549 cells. A549 cells were seeded in a 96-well plate (90 μL per well) overnight and TPAD suspensions with different concentrations (20, 40, 60, 80, and 100 μg mL^{-1}) were then added. The cells were cultivated for 24 h, and 20 μL of 1 mg/mL MTT solution was then added to each seeding well. After all cells were incubated for 4 h, the culture medium was discarded, and 150 μL DMSO solution was added. The resulting mixture was shaken for 15 min in dark at room temperature, and its optical density (OD) was measured on a microplate reader (Thermo TY10FC, USA).

2.5. Cellular Imaging

Human A549 cells were cultured in Dulbecco's modified Eagle's medium (DMEM) supplemented with 10% fetal bovine serum and 1% penicillin in humidified environment of 5% CO_2. For living cell imaging experiments of probe TPAD, cells were incubated with 20 μg mL^{-1} of probe TPAD (with 20% DMSO, v/v) for 30 min at 37 □, after incubation for 24 h, the cells washed three times with prewarmed PBS, and then imaged using an excitation wavelength of 488 nm.

3. Results and discussion

3.1. pH effect studies

Effect of pH on the fluorescence response behavior of probe TPAD was investigated with pH ranging from 1.0 to 13.0 in DMSO-PBS solution. As displayed in Fig. 1, no obvious fluorescence change could be observed for TPAD over a range of pH from 7.0 to 10.0, demonstrating that probe TPAD could be utilized over a relatively wide pH range. In consideration of the decomposition property of OCl^- in strongly acidic conditions and make sure the only ionic species presenting in the solution was OCl^-,[31] physiological pH at 7.4 was chosen for all the following experiments.

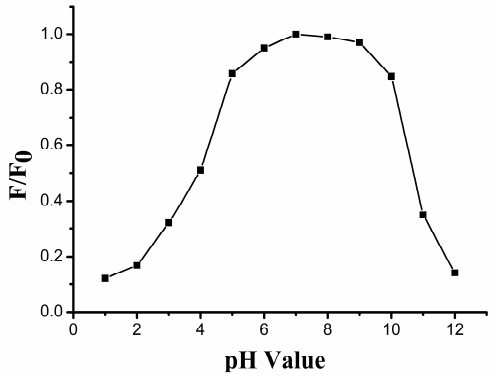

Fig. 1. PL intensity ratio (F/F_0) of TPAD at various pH values.

3.2. Selectivity studies

Selectivity experiments were conducted, where TPAD (10 mM) was subjected to various ROS species (50 μM) including H_2O_2, $TBuO^-$, HO^-, $^1O_2$, Cl^-, $ONOO^-$, NO_2^-, $H_2PO_4^-$, HCO_3^-, CO_3^{2-} and OCl^-, respectively, under the same test conditions. As shown in Fig. 2, all the selected ROS did not cause significant fluorescence change except for OCl^-, suggesting that probe TPAD possessed a good selectivity towards OCl^- against other competing species.

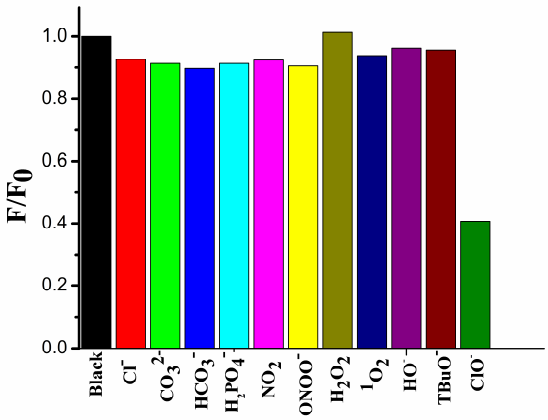

Fig. 2. Emission intensity ratio (F/F_0) of TPAD (10 mM) in aqueous conditions (PBS buffer, 20% DMSO as a co-solvent at pH 7.4) in the presence of various species (50 μM).

3.3. Photophysical property studies

From UV-vis absorption spectrum in Fig. 3, TPAD exhibited two obvious absorption bands around 310 nm and 380 nm, which were ascribed to thetriphenylamine and picolinohydrazide unit, respectively. Upon the addition of OCl

$^-$, obvious blue-shift phenomenon appeared, indicating that the conjugated structure of TPAD was wrecked. Subsquently, fluorescence titration experiments were performed to evaluate the sensing behavior of TPAD to OCl^-. As shown in Fig. 4a, the as-prepared TPAD exhibited a characteristic fluorescence emission band at 523 nm under the excitation at 375 nm. Upon the addition of various concentrations of OCl^- to TPAD solution, obvious 'turn-off' fluorescence quenching response could be observed. The relationship of fluorescence intensities in the presence of OCl^- can be exhibited in Fig. 4b with a linear equation Y = -0.011X + 0.973, R^2 = 0.992. Moreover, the detection limit (3σ) for OCl^- was calculated to be as low as 0.8 μM. Interference experiment was also performed and illustrated in Fig.5 and Fig.S4, which demonstrated that the specific fluorescence response of TPAD towards OCl^- was not disturbed by the competitive ROS species (H_2O_2, $TBuO^-$, HO^-, $^1O_2$, Cl^-, $ONOO^-$, NO_2^-, $H_2PO_4^-$, HCO_3^- and CO_3^{2-}).

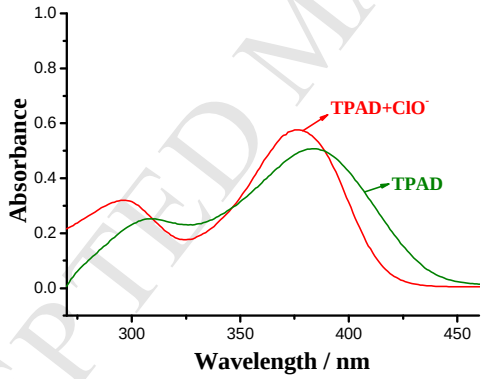

Fig. 3. UV-vis spectra of TPAD and TPAD+ClO-.

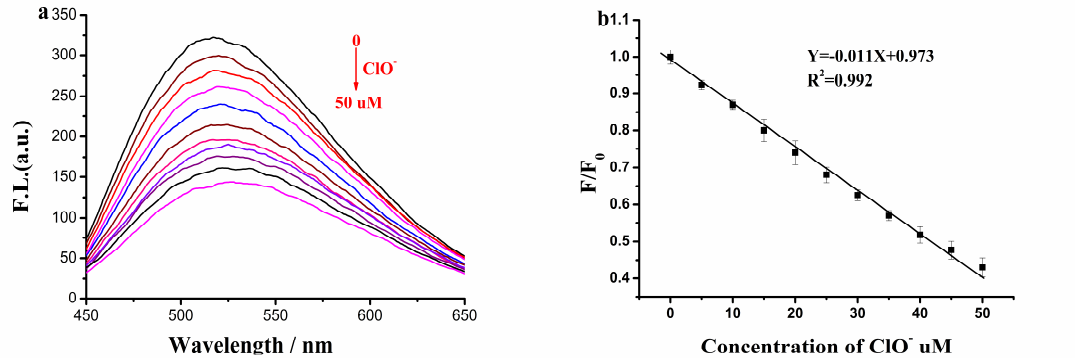

Fig. 4. (a) Fluorescence response of TPAD (10 mM, PBS buffer, 20% DMSO as a

co-solvent at pH 7.4) in the presence of increasing concentration of OCl^- (from up to down the concentration of OCl^- is 0, 5, 10, 15, 20, 25, 30, 35, 40, 45 and 50 μM). (b) The relationship of F/F_0 versus the concentration of OCl^- over the range from 0 to 50 μM (λ_{ex}=375 nm).

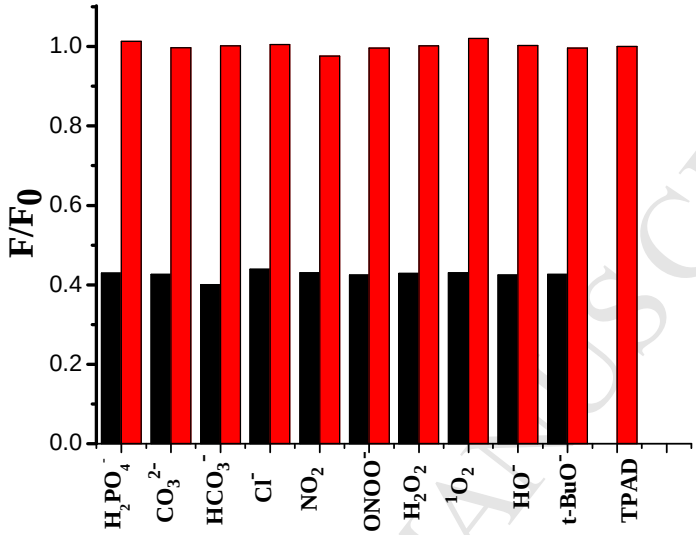

Fig. 5. The competitive selectivity of TPAD for ClO^- was examined in the presence of other ROS (50 μM). Red bars represent the addition of a single analyte including 50 μM of ROS (None, $TBuO^-$, HO^-, $^1O_2$, H_2O_2, $ONOO^-$, NO_2^-, Cl^-, HCO_3^-, CO_3^{2-} and $H_2PO_4^-$, respectively). Black bars represent the subsequent addition of ClO- (50 μM) to the mixture. All experiments were performed in PBS buffer (10 mM, pH 7.4) with 20% DMSO.

3.4. Response time studies

Response behavior of TPAD towards OCl^- was analyzed by monitoring the fluorescence changes of the reaction mixture. As showed in Fig. 6, in the absence of OCl^-, TPAD exhibited no visible variations, suggesting that probe TPAD was stable in the assay conditions. Interestingly, upon addition of OCl^-, dramatic fluorescence changes were observed and completed within 30 s. Compared with the other reported ClO^- probes (Table.S1), probe TPAD showed shorter response time, which enables the probe TPAD to facilitate real-time detection of OCl^- level changing.

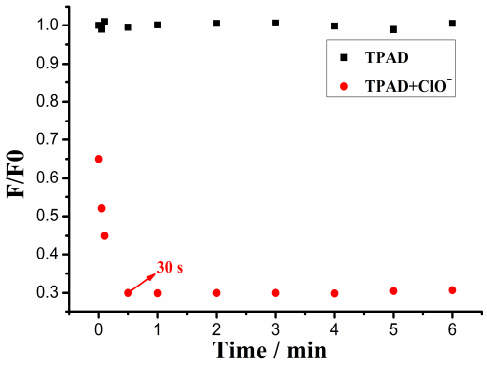

Fig. 6. Reaction-time profile of TPAD (10 mM) in the absence and presence 50 μM OCl^- in aqueous conditions in DMSO–water solution (1 : 4, v/v, 50 mM PBS buffer solution at pH 7.4). Kinetic studies were performed at ambient temperature.

3.5. The study on sensing mechanism

In order to study the reaction mechanism between TPAD and OCl^-, ^1H NMR titration experiment through adding NaOCl to a DMSO-d_6 solution of probe TPAD was carried out. Upon the addition of OCl^- species, the signal peak of characteristic proton (-CH=N) of probe TPAD at 8.56 ppm gradually decreased until disappeared, while a new signal peak at 9.77 ppm assigned to -CHO proton was observed, which demonstrated that the addition of hypochlorite triggered the conversion of imine group to the aldehyde group (Fig. 7). Furthermore, MS analysis in probe TPAD treated with OCl^- was also performed, where the mass peak at m/z = 273.95 corresponding to product was observed (Fig. S5). UV-vis absorption spectrum also proved the reliability of the mechanism indirectly. There is a π-π conjugated structure in probe TPAD with good fluorescence properties. After the addition of OCl-, the C=N double bond of TPAD was destroyed and the raw material molecule was released which results in conjugate degree descent and the blue shift phenomenon for TPAD from UV-vis spectrum. These results supported the proposed sensing mechanism, which was shown in Scheme 2.

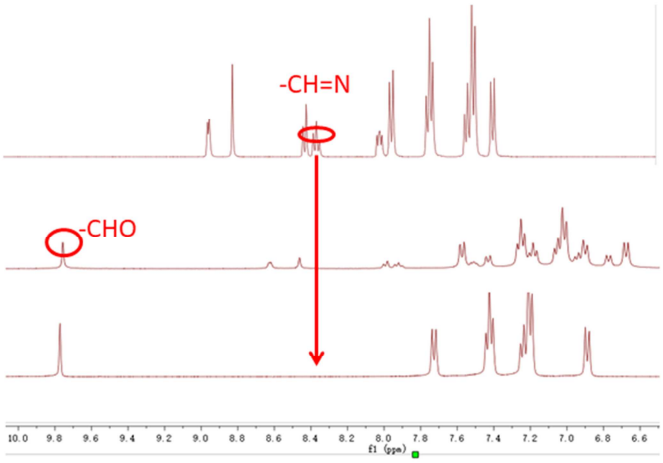

Fig.7. Partial ^{1}H NMR spectra of probe **TPAD,** probe **TPAD** + 10 μM OCl^- and **TPAD** + 50 μM OCl^- in DMSO-d_6.

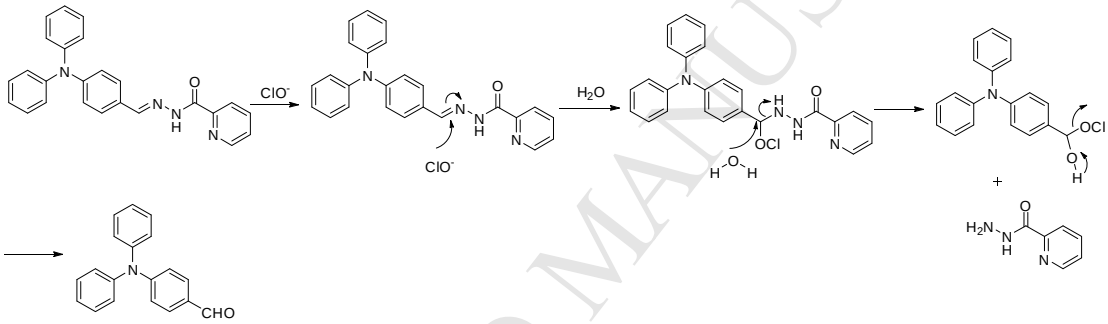

Scheme. 2 Proposed sensing mechanism of probe TPAD in response to OCl^-.

3.6. Cell imaging

Bioimaging application was assessed using TPAD as a fluorescent probe for OCl^- detection in living cells. MTT assay was firstly carried out to evaluate the cytotoxicity of the TPAD to A549 cells. As illustrated in Fig. S6, the viability of A549 cells declined no less than 8% while the TPAD concentration increasing up to 100 μg/mL, which indicated that the TPAD concentration in vitro is much higher than that of required for the imaging of living cells. Furthermore, the bioimaging applicability of TPAD was evaluated using a Nikon confocal laser scanning microscope. As shown in Fig. 8, strong green fluorescence in living A549 cells was observed after the cells were incubated with TPAD. Subsequently, after incubated with OCl^- (50 μM) for 8 h, the channel green fluorescence was found to be invisible. These results revealed that probe TPAD was able to effectively detect OCl^- in living cells.

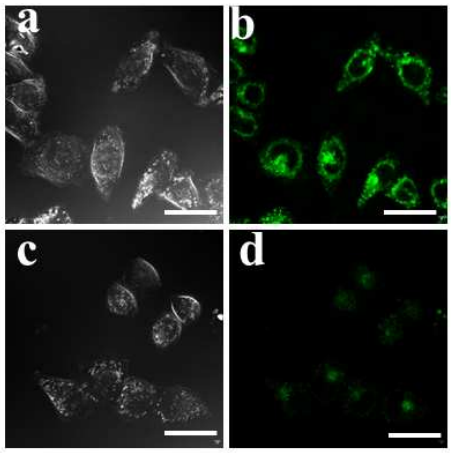

Fig. 8. Confocal fluorescence images of A549 cells. (a, c) A549 cells incubated with the TPAD (10 mM) and TPAD + OCl^- (50 μM); (b) TPAD fluorescence image in the green channel; (d) TPAD+OCl^- (50 μM) fluorescence image in the green channel (scale bar: 10 μm).

4. **Conclusions**

In summary, we have developed a novel probe TPAD for OCl^- detection by expediently combining benzaldehyde and picolinate units. The probe TPAD exhibited excellently selective response towards OCl^- over potentially competing reactive oxygen species with rapid response time (30 s). In addition, fluorescent imaging analysis showed that TPAD could be used to detect OCl^- in biological systems with high sensitivity and excellent biocompatibility. The specific detection of OCl^- provides novel sight into the reactive-type fluorescent probe and would be of great benefit for exploiting new functions and mechanisms of OCl^- sensing in living systems.

Acknowledgement

This work was supported the China Postdoctoral Fund Surface Project (2017M610335), Fundamental Research Funds of Jiangsu Key Lab. of Biomass Energy and Material (JSBEM-S-201806) and a Project Funded by the Priority Academic Program Development of Jiangsu Higher Education Institutions (PAPD).

Appendix A. Supplementary data

Supplementary data associated with this article can be found, in the online

version, at http://dx.doi.org/10.1016/j.tet.2018.XX.XX.

Notes and references

[1] D. T. Quang, J. S. Kim, Chem. Rev., 2011,**133**, 6280-6301.

[2] A. Manke, S. Luanpitpong, C. Dong, L. Wang, X. He, L. Battelli, R. Derk, T. Stueckle, D. Porter, T. Sager, H. Gou, C. Dinu, N. Wu, R. Mercer, Y. Rojanasakul, Int. J. Mol. Sci., 2014,**15**, 7444-7461.

[3] J. L. Fan, H. Y. Mu, H. Zhu, J. Y. Wang, X. J. Peng, Analyst, 2015, **140**, 4594-4598.

[4] D. I. Pattison, C. L. Hawkins, M. J. Davies, biochemistry, 2007, **46,** 9853-9864.

[5] D. I. Pattison, M. J. Davies, Chem. Res. Toxicol., 2001, **14**, 1453-1464.

[6] W. Y. Lin, L. L. Long, Chem. Eur. J., 2009, **15**, 2305-2309.

[7] Y. Koide, Y. Urano, K. Hanaoka, T. Terai, T. Nagano, J. Am. Chem. Soc., 2011, **133**, 5680-5682.

[8] A. Daugherty, J. L. Dunn, D. L. Rateri, J. W. Heinecke, J. Clin. Invest., 1994, **94**, 437-444.

[9] M. Benhar, D. Engelberg, A. Levitzki, EMBO Rep., 2002, **3**, 420-425.

[10] J. Shi, Q. Q. Li, X. Zhang, M. Peng, J. G. Qin, Z. Li, Sens. Actuators B, 2010, **145**, 583-587.

[11] D. Pattison, M. Davies, Biochemistry, 2006, **45**, 8152-8162.

[12] Y. K. Yue, F. J. Huo, C. X. Yin, O. E. Jorge, M. S. Robert, Analyst, 2016, **141**,1859-1873.

[13] R.X. Ji, K. Qin, A. K. Liu, Y. Zhu, Y. Q. Ge, Tetrahedron Lett., 2018, **59** , 2372-2375.

[14] Y. L. Wu, J. Wang, F. Zeng, S. L. Huang, J. Huang, H. T. Xie, C. M. Yu, S. Z. Wu, ACS Appl. Mater. Interfaces, 2016, **8**, 1511-1519.

[15] Q. Xu, P. Pu, J. Zhao, C. Dong, C. Gao, Y. Chen, J. Chen, Y. Liu, H. Zhou, J. Mater. Chem. A,2015, **3**, 542-546.

[16] K. Sreenath, Z. Yuan, J. R. Allen, M. W. Davidson, L. Zhu, Chem. Eur. J., 2015, **21**, 867-874.

[17] Y. W. Jun, S. Sarkar, S. Subhankar, Y. J. Reo, H. R. Kim,J. J. Kim, Y. T. Chang, K. H. Ahn, Chem. Commun., 2017, **53**, 10800-10803.

[18] L. L. Long, Y. J. Wu, L. Wang, A. H. Gong, F. L. Huc, C. Zhang, Chem. Commun., 2015, **51**, 10435-10438.

[19] J. J. Hu, N. K. Wong, Q. S. Gu, X. Y. Bai, S. Ye ,D. Yang, Org. Lett., 2014, **16**, 3544-3547.

[20] J. Shi, Q. Q. Li, X. Zhang, M. Peng, J. G. Qin, Z. Li, Sens. Actuators, B, 2010, **145**, 583-587.

[21] S. R. Liu, M. Vedamalai, S. P. Wu, Anal. Chim. Acta, 2013, **800**, 71-76.

[22] Q. L. Xu, K. A. Lee, S. Y. Lee, K. M. Lee, W. J. Lee , J. Y. Yoon, J. Am. Chem. Soc., 2013, **135**, 9944-9949.

[23] X. Q. Chen, K. A. Lee, X. T. Ren, J. C. Ryu, G. M. Kim, J. H. Ryu, W. J. Lee, J. Y. Yoon, Nat. Protoc.,2016, **7**, 1219-1228.

[24] J. W. Li, C. X. Yin, F. J. Huo, K. M. Xiong, J. B. Chao, Y. B. Zhang, Sens. Actuators B , 2016, **231**, 547-551.

[25] Y. Zhou , W. B. Pei , C. Y. Wang , J. X. Zhu , J. S. Wu , Q. Y. Yan ,L. Huang , W. Huang , C. Yao , S. C. l. Joachim, Q. C. Zhang, Small, 2014, **17**, 3560-3567.

[26] X. H. Zhou, Y. R. Jiang, X. J. Zhao, D. Guo, Talanta, 2016, **160**, 470-474.

[27] P. Agarwala, D. Kabra, J mater. Chem. A, 2017, **4**, 1348-1373 .

[28] X. J. Lian, Z. Zhao, D. J. Cheng, Mol. Cryst. Liq. Cryst., 2017, **1**, 223-235.

[29] H. Yan, X. L. Meng, B. Y. Li, S. S. Ge, Y. Lu, Dyes Pigments, 2017, **146**, 479-490.

[30] F. J. Huo, Y. Q. Zhang, J. Kang, J. B. Chao, Y. B. Zhang, C. X. Yin, Sens. Actuators B , 2017, **243**, 429-434.

[31] Y. L. Jiang, S. S. Wu, C. Jin, B. X. Wang, J. Shen, Sens. Actuators B , 2018, **265**, 365-370.